

Similar glassy features in the ^{139}La NMR response of pure and disordered $\text{La}_{1.88}\text{Sr}_{0.12}\text{CuO}_4$

V. F. Mitrović,^{1,2} M.-H. Julien,^{3,*} C. de Vaulx,³ M. Horvatić,¹ C. Berthier,¹ T. Suzuki,⁴ and K. Yamada⁵

¹Grenoble High Magnetic Field Laboratory, CNRS, Boîte Postale 166, 38042 Grenoble Cedex 9, France

²Department of Physics, Brown University, Providence, Rhode Island 02912, USA

³Laboratoire de Spectrométrie Physique, UMR5588 CNRS and Université Joseph Fourier-Grenoble, 38402 Saint-Martin-d'Hères, France

⁴Advanced Meson Science Laboratory, Nishina Center, RIKEN, 2-1 Hirosawa, Wako, Saitama 351-0198, Japan

⁵Institute for Materials Research, Tohoku University, Katahira 2-1-1, Sendai, 980-8577, Japan

(Received 8 February 2008; revised manuscript received 13 May 2008; published 8 July 2008)

High T_c superconductivity in $\text{La}_{2-x}\text{Sr}_x\text{CuO}_4$ coexists with (striped and glassy) magnetic order. Here, we report NMR measurements of the ^{139}La spin-lattice relaxation, which displays a stretched-exponential time dependence, in both pure and disordered $x=0.12$ single crystals. An analysis in terms of a distribution of relaxation rates $^{139}\text{T}_1^{-1}$ indicates that: (i) the spin-freezing temperature is spatially inhomogeneous with an onset at $T_g^{\text{onset}}=20$ K for the pristine samples and (ii) the width of the T_1^{-1} distribution in the vicinity of T_g^{onset} is insensitive to an $\sim 1\%$ level of atomic disorder in CuO_2 planes. This suggests that the stretched-exponential ^{139}La relaxation, considered as a manifestation of the system's glassiness, may not arise from quenched disorder.

DOI: 10.1103/PhysRevB.78.014504

PACS number(s): 74.25.Ha, 74.72.Dn, 75.10.Nr

I. INTRODUCTION

The coexistence of magnetic order with superconductivity is a prominent feature of $\text{La}_{2-x}\text{Sr}_x\text{CuO}_4$ (Ref. 1) and other underdoped high T_c cuprates,^{2,3} even in zero magnetic field. However, neither the origin of this static magnetism nor the reason for its glassy character is fully understood. An important school of thought focuses on stripe physics.⁴ Indeed, the temperature of magnetic freezing, T_g , in $\text{La}_{2-x}\text{Sr}_x\text{CuO}_4$ is peaked in the vicinity of $x \approx \frac{1}{8}$ (Fig. 1), and neutron-scattering studies⁵⁻⁷ reveal long-range antiferromagnetic order with the same typical modulation as in the materials presenting direct evidence for charge-stripe order.⁸ Another approach relies on electronic and magnetic inhomogeneities generated by quenched disorder.⁹ Undoped or weakly hole-doped droplets may form the magnetic clusters which freeze at low temperature, as suggested by the recent nuclear-magnetic-resonance (NMR) evidence for a nanoscale inhomogeneity of the hole concentration in $\text{La}_{2-x}\text{Sr}_x\text{CuO}_4$.¹⁰ Furthermore, the importance of quenched disorder could be supported by the glassy features observed in superconducting samples ($x \geq 0.06$).¹ These are reminiscent of the spin-glass behavior, well documented for $0.03 \leq x \leq 0.05$. Spatial heterogeneity is particularly evident in a number of magnetic measurements, such as the stretched-exponential NMR relaxation of ^{139}La nuclei. This heterogeneity develops as the magnetic fluctuations slow down over a substantial temperature range on cooling above the freezing temperature T_g , the value of which depends on the time scale of the measuring probe. These properties are typical of glassy systems.

Glassiness is, however, also present in materials where stripe order is well defined and relatively long range.⁸ Furthermore, from the T dependence of an average ^{139}La spin-lattice relaxation rate T_1^{-1} , Curro *et al.*¹¹ concluded that the distribution of magnetic correlation times is similar in several materials with very different hole or impurity contents. This has led to the suggestion that glassiness in these mate-

rials is not due to quenched disorder but is self-generated by the charge stripes.¹² Later, Hunt *et al.*¹³ determined the distribution of correlation times in stripe-ordered materials in a more direct way than Curro *et al.*¹¹ did, i.e., from the recovery of the ^{139}La NMR signal. The stretched-exponential re-

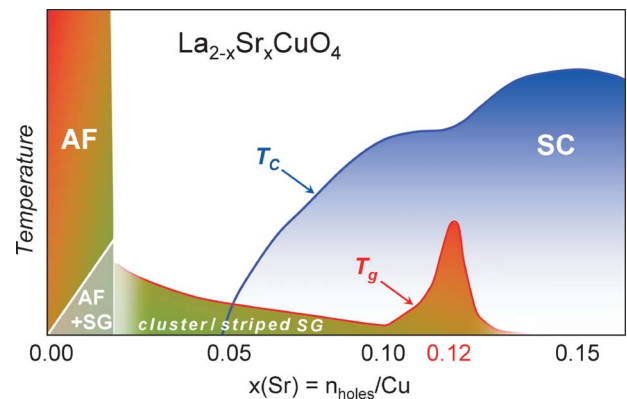


FIG. 1. (Color online) Sketch of the phase diagram of $\text{La}_{2-x}\text{Sr}_x\text{CuO}_4$. AF denotes antiferromagnetic; SC, superconducting; and SG, spin-glass phase. T_g defines the temperature of the transition to the frozen state which has been named as “cluster spin glass” before the discovery of stripes (see Ref. 1 and references therein). T_g is defined from either NMR or μSR measurements. These two low-energy magnetic probes of comparable (though not necessarily identical) time scales give similar values of T_g , enabling one to obtain a coherent phase diagram (Ref. 1). Remarkably, T_g (together with the spin stiffness—see text) is enhanced for $x \approx 0.12$. One of the questions regarding the cluster spin-glass phase is whether the nonmonotonic behavior of T_g vs x suggests that the physics for $x \approx 0.12$ is different from that for $x \leq 0.10$. Note that the main difference between $\text{La}_{2-x}\text{Sr}_x\text{CuO}_4$ and compounds presenting direct evidence for charge-stripe order (e.g., $\text{La}_{2-x}\text{Ba}_x\text{CuO}_4$) is that the peak of T_g vs x around $x \approx 0.12$ is considerably wider in these latter compounds (Ref. 3).

laxation was thus better characterized, but its origin was not the focus of the discussion.

In this paper, we report ^{139}La NMR measurements in $\text{La}_{1.88}\text{Sr}_{0.12}\text{CuO}_4$, where T_g is maximum, as illustrated in Fig. 1. We quantify the ^{139}La stretched-exponential relaxation and discuss the issues of inhomogeneity and atomic disorder.

II. SAMPLES

Single crystals, with typical size of $2 \times 3 \times 4$ mm³, were cut from rods grown by the traveling solvent floating zone method. Growth at a rate of ≈ 1 mm/h yielded “pristine” samples with the standard T_c of 30 K,⁵ while growth at 0.2 mm/h produced a “disordered” sample with a low T_c of 10 K ($T_c^{\text{onset}} = 12$ K).¹⁴ Neutron-scattering (NS) studies have shown that the two crystals have the same structure as well as an identical temperature of the transition from the high T tetragonal (HTT) phase to the low T orthorhombic (LTO) phase. These studies have also revealed an identical incommensurability of the magnetic peaks. Since these quantities depend strongly on x , the results demonstrate that the two crystals have the same doping $x=0.12$. On the other hand, magnetic Bragg peaks appear below $T_g^{\text{NS}} = 30$ K (Ref. 5) and 25 K (Ref. 14) for the pristine and disordered samples, respectively. All of these properties, as well as an upturn of the zero-field in-plane resistivity below 80 K, are consistent with the presence of $\sim 1\%$ of nonmagnetic defects in the disordered sample.¹⁵ These defects likely correspond to Cu vacancies, which produce the same magnetic effects as nonmagnetic impurities.^{16,17}

III. NMR METHODS

As done in Ref. 18, the applied magnetic field was tilted away from the c axis by $\theta \sim 10^\circ$ in order to obtain a sharp peak on the high-frequency edge of the ^{139}La central, $\langle +\frac{1}{2} \leftrightarrow -\frac{1}{2} \rangle$, Zeeman transition. T_1 was measured on this peak, shown as a shaded part of the sample spectra in the inset of Fig. 2. The T dependence of T_1 is identical on other peaks in the central transition spectrum. Experiments were performed in fields of 9 T (for $x=0.12$, $T_c=10$ K sample) and 14 T (for $x=0.12$, $T_c=30$ K and $x=0.10$ samples).

In Fig. 2, we plot the temperature dependence of ^{139}La linewidth for the high-frequency peak (shaded region in the inset) of $\langle +\frac{1}{2} \leftrightarrow -\frac{1}{2} \rangle$ transition for $\text{La}_{1.88}\text{Sr}_{0.12}\text{CuO}_4$ ($T_c=30$ K sample). The linewidth broadens with decreasing temperature, indicating increasing distribution of local static magnetization as the temperature is lowered.

We remark that even at the lowest T , the signal from other central transition lines is insignificant at the frequency of the high-frequency peak and its high-frequency side for this orientation of the applied field. Therefore, the temperature evolution of the measured relaxation rates is intrinsic to magnetism and not a result of signal overlap from other central transition lines.

We also point out that no sign of phase separation is detected in our NMR data, in apparent disagreement with muon spin resonance (μSR) data showing a magnetic volume fraction of $\sim 20\%$ for $x=0.12$.¹⁹ Since NMR was performed here

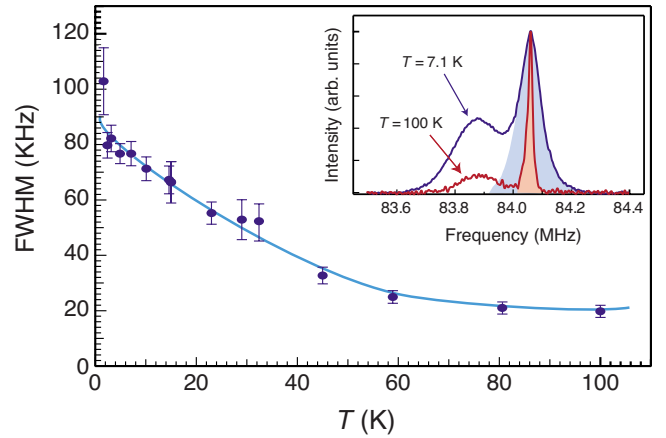


FIG. 2. (Color online) The temperature dependence of ^{139}La linewidth (filled symbols) for the high-frequency peak (shaded region in the inset) of $\langle +\frac{1}{2} \leftrightarrow -\frac{1}{2} \rangle$ transition in the magnetic field applied at $\theta \sim 10^\circ$ away from the c axis for $\text{La}_{1.88}\text{Sr}_{0.12}\text{CuO}_4$ ($T_c=30$ K sample). The solid line is a guide for the eyes. Inset: Normalized spectra at $T=100$ K and $T=7.1$ K as denoted. The shaded areas mark the high-frequency peak where the rates presented here are determined. The low-frequency peak contains the signal from other quadrupolarly split $\langle +\frac{1}{2} \leftrightarrow -\frac{1}{2} \rangle$ transition lines (Ref. 18).

in a high magnetic field, part of the discrepancy might be resolved by an increase in the magnetic volume fraction with the applied field.^{20,21}

IV. ANALYSIS OF T_1 DATA

In Fig. 3, we display the time (t) dependence of the ^{139}La longitudinal magnetization $\mathcal{M}(t) = M_z(t)/M_z(\infty)$ after a comb of $\frac{\pi}{2}$ saturation pulses in the pristine sample. Clearly, the data cannot be fitted by the theoretical formula,²² which corresponds to $\alpha=1$ (“exponential” relaxation) in

$$\mathcal{M}_\alpha(t, T_1^{-1}) = 1 - 0.714e^{-(28t/T_1)^\alpha} - 0.206e^{-(15t/T_1)^\alpha} - 0.068e^{-(6t/T_1)^\alpha} - 0.012e^{-(t/T_1)^\alpha}. \quad (1)$$

We point out that the above statement is true for data at any temperature below ≈ 80 K, as evident in Fig. 3(c), when $\alpha < 1$. In $\text{La}_{2-x}\text{Sr}_x\text{CuO}_4$ materials, the stretched relaxation, i.e., the deviation from $\mathcal{M}_{\alpha=1}(t, T_1^{-1})$, has been attributed to the distribution of ^{139}La T_1^{-1} values. We shall comment on this interpretation below.

In an ideal case, one-to-one correspondence between dynamic and static inhomogeneities can be revealed by measuring T_1^{-1} as a function of position across the NMR line shape (see Refs. 10 and 23 for example). However, despite the observation of a continuous line broadening (shown in Fig. 2), no significant frequency dependence of T_1^{-1} was found across the ^{139}La line. Thus, to quantify the inhomogeneities, one must resort to alternative analysis of $\mathcal{M}(t)$ data, in two possible ways:

(i) First, a fit to Eq. (1) is made with the stretching exponent $\alpha \neq 1$. This provides a phenomenological account of the distribution of T_1 values (Fig. 3).

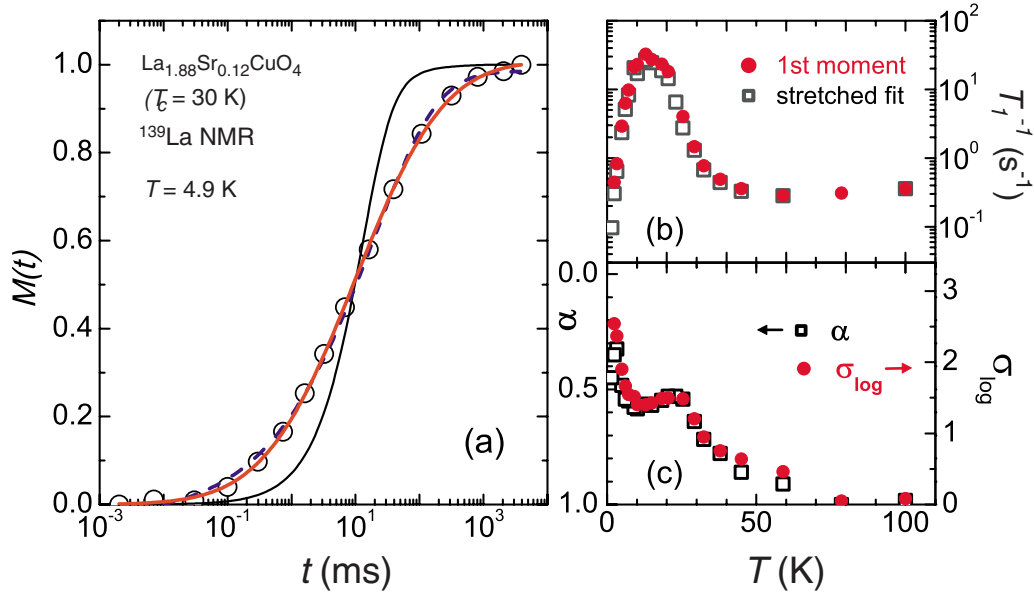


FIG. 3. (Color online) (a) An example of the time dependence of the ^{139}La normalized longitudinal magnetization $\mathcal{M}(t)=M_z(t)/M_z(\infty)$ after saturation of the central transition (dots) in $\text{La}_{1.88}\text{Sr}_{0.12}\text{CuO}_4$ ($T_c=30$ K sample). The thin black line is a fit to Eq. (1) with $\alpha=1$. The blue (dark gray) dashed line is a fit to Eq. (1) with $\alpha=0.48$. The thick red (light gray) line is the fit to Eq. (2). [(b) and (c)] Comparisons of results obtained from the stretched-exponential fit (open symbols) and from the Gaussian distribution fit (filled symbols). See text for details.

(ii) Second, the formula $\mathcal{M}_{\alpha=1}(t, T_1^{-1})$ is convoluted with a chosen probability distribution function of T_1^{-1} . We found that a good fit to the data is provided by the Gaussian distribution on a logarithmic ($\log_{10} T_1^{-1}$) scale:

$$\mathcal{M}_G(t) = (\sqrt{\pi/2}\sigma_{\log})^{-1} \int e^{-2(\log_{10} R_1 - \log_{10} T_1^{-1})^2 / \sigma_{\log}^2} \times \mathcal{M}_{\alpha=1}(t, R_1) d(\log_{10} R_1). \quad (2)$$

This fit is defined by only two parameters: the most probable relaxation rate T_1^{-1} (i.e., the center of the Gaussian) and the width of the distribution σ_{\log} on a \log_{10} scale. Using the $\log_{10} T_1^{-1}$ space is more physical when very broad distributions of relaxation rates are expected. This also naturally avoids the introduction of an artificial low T_1^{-1} cutoff needed to eliminate unphysical negative values encountered when the linear scale is used. The fit yields T_1^{-1} values equivalent to the stretched fit $\mathcal{M}_{\alpha}(t, T_1^{-1})$, as confirmed from the analysis of our data shown in Fig. 3(b). Furthermore, the value of σ_{\log} directly shows over how many orders of magnitude the distribution of relaxation rates is spread. Direct insight into this parameter is the main advantage of this fit (see Fig. 4). σ_{\log} also appears to be linearly related to the value of α , as demonstrated in Fig. 3(c), in agreement with predictions of the recent theoretical work of Johnston²⁴ for $\alpha \geq 0.5$. We also remark that we cannot experimentally determine the unique/exact shape of the distribution function. Equally good fits of the data can be achieved by assuming, e.g., an asymmetric Gaussian or a Lorentzian distribution for T_1^{-1} . Thus, we choose to analyze the data by assuming a distribution function of the simplest form, a Gaussian. However, the results to be discussed below have been found to be insensitive to the choice of the exact form of the distribution.

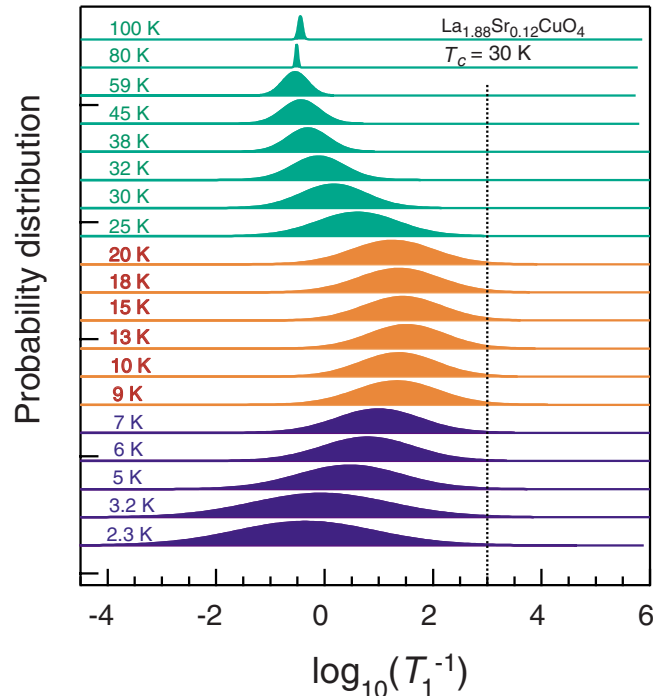


FIG. 4. (Color online) The Gaussian probability distribution of the relaxation rate as a function of T for $\text{La}_{1.88}\text{Sr}_{0.12}\text{CuO}_4$ ($T_c=30$ K sample). The rates are in units of s^{-1} . The amplitudes of distributions are normalized to 1 and the curves are offset for clarity. The vertical line indicates a typical maximum value $(T_1^{-1})_{\max} \approx 10^3 \text{ s}^{-1}$ in the system. Green (lightest gray) depicts the T interval (from 100 to 25 K) of slowing down; red (lighter gray) represents the T range (from 20 to 9 K) where spins freeze throughout the sample; and navy blue (dark gray) is used when all of the sample is magnetically frozen on the NMR time scale.

V. TEMPERATURE DEPENDENCE OF THE SPIN DYNAMICS

In this section, we shall first give a qualitative description of the temperature dependence of the mean relaxation rate T_1^{-1} in order to define the freezing temperature T_g on the time scale of NMR. Then, tentative fits of the T dependence of T_1^{-1} will be described. This parametrization of the data enables primarily a comparison between different $\text{La}_{2-x}\text{Sr}_x\text{CuO}_4$ samples, although it cannot provide a physical picture of the spin-glass freezing in the system. Furthermore, the shortcomings of such analysis based on the mean value of the distribution of T_1^{-1} values are alluded to in Sec. VI.

The temperature dependence of T_1 may be understood, at least qualitatively, from the following expression:

$$\frac{1}{T_1} = \gamma_n^2 \langle h_\perp^2 \rangle \frac{2\tau_c}{1 + \omega_n^2 \tau_c^2}, \quad (3)$$

where τ_c is the correlation time, $h_\perp = (h_{xx}^2 + h_{yy}^2)^{1/2}$ is the component of the hyperfine field perpendicular to the field direction, and ω_n is the NMR frequency.²⁵ At high temperatures the correlation time is short; that is, the condition $\tau_c^{-1} \gg \omega_n$ is satisfied. As the dynamics of the system slows down upon cooling, τ_c^{-1} decreases, causing an increase in T_1^{-1} . This occurs down to the temperature T_g^{NMR} , at which the condition $\tau_c^{-1} = \omega_n$ is reached.²⁶ Upon further cooling, τ_c^{-1} continues to decrease but T_1^{-1} decreases. Thus, T_g^{NMR} , the temperature of freezing on the time scale of ^{139}La NMR ($\omega_n \approx 10^8$ Hz), is defined as the temperature at which the relaxation rate is at its maximum value:

$$(T_1^{-1})_{\text{max}} \equiv T_1^{-1}(T_g^{\text{NMR}}) = \gamma_n^2 \langle h_\perp^2 \rangle \omega_n^{-1}. \quad (4)$$

For our pristine $x=0.12$ sample, the peak of the mean T_1^{-1} occurs at $T_g^{\text{NMR}} = 13$ K. The temperature at which the increase of T_1^{-1} becomes noticeable may be defined as $T^{\text{slow}} = 45$ K. Interestingly, the ratio $T^{\text{slow}}/T_g^{\text{NMR}} \approx 3.5 \pm 0.5$ is much lower for $x=0.12$ than for $x=0.10$ ($T^{\text{slow}}/T_g^{\text{NMR}} \approx 7.4$) and for other values of x .^{27,28} This statement holds even if an onset T_g^{NMR} is considered, as described in Sec. VI. Note also that the ratio is believed to be magnetic field independent for the fields ($H_0 \leq 14$ T) investigated here.¹⁸

A more quantitative approach requires an analysis of the temperature dependence of T_1 . Although it is not clear on which theoretical model such an analysis should be based, two models which have been used in the context of spin-freezing in the cuprates can be used.

First, we use Eq. (3) with an activated correlation time $\tau_c = \tau_0 \exp(E_a/k_B T)$ to fit the temperature dependence of ^{139}Tl data with τ_0 and E_a as fitting parameters, as depicted in Fig. 5. This fit allows extraction of the effective ‘‘energy barrier’’ (E_a) for the activation of a thermally driven spin-freezing process. Fitting the data for $T_g^{\text{NMR}} < T < T^{\text{slow}}$, we find the effective energy barrier $E_a = 140 \pm 30$ K for our pristine $x=0.12$ sample. This value is to be compared with $E_a = 84 \pm 20$ K for the disordered $x=0.12$ sample and $E_a = 13 \pm 3$ K for $x=0.10$.

Another possibility is to use the renormalized classical form²⁹ of the two-dimensional (2D) Heisenberg model on a square lattice, which also captures well the increase in T_1^{-1}

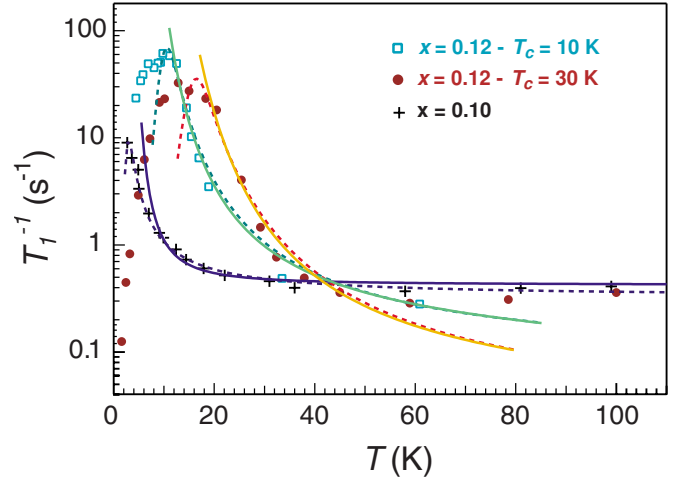


FIG. 5. (Color online) Fits to the relaxation rate T_1^{-1} data as plotted in Fig. 6(a). The dashed lines are fits to Eq. (3) with $\tau_c = \tau_0 \exp(E_a/k_B T)$. The solid lines are fits to Eq. (5) for both $x=0.12$ samples and to Eq. (6) for $x=0.10$, as described in the text.

with decreasing temperature above T_g^{NMR} (see also Ref. 13). This form allows extraction of the effective spin-stiffness (ρ_s) parameter. As illustrated in Fig. 5, in the temperature range $T_g^{\text{NMR}} \leq T \leq T^{\text{slow}}$, the data for both $x=0.12$ samples fit well to the low-temperature limit ($T \leq 2\pi\rho_s/2$) of the renormalized classical form, expressed as

$$\frac{1}{T_1} \propto \frac{e^{C/T}(T/C)^{3/2}}{C(1+T/C)^3}. \quad (5)$$

Here $C \equiv 2\pi\rho_s$ is a fitting parameter. We find the value of $\rho_s = 25 \pm 5$ K for the spin stiffness of our pristine $x=0.12$ sample. For the disordered $x=0.12$, a weaker value of $\rho_s = 19 \pm 4$ K is found. An even weaker value ($\rho_s = 2 \pm 1$ K) is found for the $x=0.10$ sample. This correlates with the fact that $T^{\text{slow}}/T_g^{\text{NMR}} \approx 7.4$ for this sample. Due to its weak spin-stiffness parameter, the data for the $x=0.10$ sample are fitted to the high-temperature limit ($T \geq 2\pi\rho_s/2$) of the renormalized classical form,²⁹ given by

$$\frac{1}{T_1} \propto \left(1 + \frac{C}{4T}\right)^{1/2} \exp\left[\left(1 + \frac{C}{4T}\right)\left(\frac{C}{2T}\right)^2\right], \quad (6)$$

with $C \equiv 2\pi\rho_s$ as a fitting parameter. Not surprisingly (given the similarities of the fitting formulas in this temperature range), the extracted values of the spin stiffness $2\pi\rho_s$ are comparable to the values of the effective energy barrier in all the three samples. On the other hand, the spin-stiffness values are smaller than those in La-based cuprates with low temperature tetragonal structure and charge-stripe order.^{13,30}

In conclusion, it appears that $x=0.12$ is the concentration for which the temperature range of slowing down of the magnetic fluctuations is the least extended and/or the spin stiffness is the strongest. We remark that the last point is in agreement with results in Ref. 30.

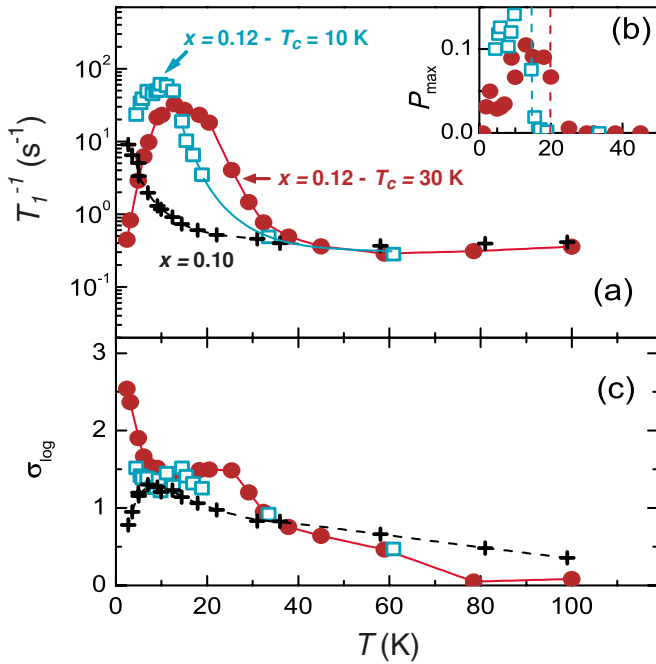


FIG. 6. (Color online) (a) ^{139}La spin-lattice relaxation rates T_1^{-1} defined as the center of the Gaussian distribution \mathcal{P} for the two $x=0.12$ samples and for an $x=0.10$ sample. (b) $P_{\max} = \mathcal{P}[\log_{10}(T_1^{-1})_{\max}] / \mathcal{P}[\log_{10}(T_1^{-1})]$ where $(T_1^{-1})_{\max} = 10^3 \text{ s}^{-1}$ (same symbol codes as those in main panel). The vertical dashed lines denote $T=15$ and 20 K, where the first spins become frozen in the samples. (c) Width σ_{\log} of $\mathcal{P}(\log_{10} T_1^{-1})$ (same symbol codes as those in upper panel). The lines are guides for the eyes. The downturn of σ_{\log} at low T for $x=0.10$ might be due to a loss of NMR signal.

VI. INHOMOGENEITY OF T_g

For a more adequate description of the spin freezing, it is in fact the maximum, and not the mean, T_1^{-1} value present in the system which should be considered. We define this value to be the rate at which the probability distribution is 1% of its maximum. Based on results shown in Figs. 4 and 6(b), we deduce that a typical maximum value is approximately $(T_1^{-1})_{\max} \approx 10^3 \text{ s}^{-1}$. It is apparent in Fig. 6(b) that the weight of the Gaussian distribution at $T_1^{-1} = 10^3 \text{ s}^{-1}$ becomes sizable at $T_g^{\text{NMR}}(\text{onset}) = 20$ K. This means that spins begin to be frozen well above 13 K in some regions of the sample. Our $T_g^{\text{NMR}} = 20$ K agrees perfectly with the appearance of a coherent precession of the muon spin in an $x=0.12$ single crystal similar to ours.¹⁹

Here, it must be recognized that $(T_1^{-1})_{\max} = 10^3 \text{ s}^{-1}$ probably also represents a cut-off value above which the ^{139}La NMR signal is unobservable (wipe-out phenomenon).^{11,13,18} However, the consistency of the above analysis³¹ suggests that our data correctly describe the spin dynamics of the system at least down to 20 K.

For the disordered sample, the freezing occurs at a lower temperature: T_1^{-1} vs T shows a peak at $T=10$ K and $T_g^{\text{NMR, onset}} = 15$ K. This is consistent with the qualitative analysis discussed in Sec. V and with the decrease in T_g^{NS}

from 30 K (pristine)⁵⁻⁷ to 25 K (disordered),¹⁴ as determined by neutron scattering. Since the elastic NS signal is integrated over a typical energy window of ~ 1 meV and the slowing down of the fluctuations occurs on a relatively wide T range, we observe that $T_g^{\text{NS}} > T_g^{\text{NMR}}$.

VII. INHOMOGENEITY OF THE SPIN DYNAMICS

The distribution of T_1 values acquires a significant width only at $T \approx 60$ K and below. The fact that $\sigma_{\log} \approx 0$ at $T=80$ and 100 K is remarkable. This means that the distribution of T_1^{-1} values seen by ^{63}Cu or ^{17}O NMR at these temperatures and attributed to a nanoscale inhomogeneity of the hole concentration¹⁰ is completely absent in the ^{139}La T_1 data. This contrasting situation is explained by two facts: First, the hyperfine field at ^{139}La sites results from the coupling to several electronic sites in two different CuO_2 planes. Thus, the hyperfine field is spatially more homogeneous than the electronic density. Second, the relatively weak amplitude of this (transferred) hyperfine field produces much weaker differences in the T_1 values for ^{139}La than for ^{63}Cu or ^{17}O . Still, the ^{139}La inhomogeneity, which shows up at lower temperature, appears to be correlated with inhomogeneities in the static local magnetization, as revealed by the similar temperature dependences of both the distribution width σ_{\log} and the static ^{139}La linewidth shown in Figs. 3(c) and 2, respectively. However, for the reasons given above, no direct correlation between the inhomogeneity of ^{139}La and the resonance frequency across the ^{139}La line could be established.

Since ^{17}O and $^{63,65}\text{Cu}$ NMR signals undergo a significant wipeout below ~ 50 K,^{18,32} it is difficult to know whether the inhomogeneity probed in ^{139}La T_1 measurements below ~ 60 K is distinct from the one probed at higher temperatures and attributed to spatial variation of the hole concentration. At any given temperature below ~ 20 K, the difference in ^{139}La T_1^{-1} values between $x=0.12$ and $x=0.10$ samples exceeds an order of magnitude. However, even if the amplitude of the nanoscale doping inhomogeneity does not produce a significant effect on the ^{139}La NMR at ~ 100 K, the possibility that it produces the large ^{139}La T_1 distribution at low T cannot be discarded. On the other hand, it is possible that magnetic heterogeneity (ubiquitous in glassy systems) develops prior to the glass transition in $\text{La}_{2-x}\text{Sr}_x\text{CuO}_4$, in addition to a nanoscale electronic inhomogeneity. In support to this is the fact that spin freezing and substantial magnetic inhomogeneity are reported in $\text{YBa}_2\text{Cu}_3\text{O}_{6+x}$,² while a significant nanoscale variation of the hole concentration is apparently absent in this system.³³

As evident in Fig. 6(b), T_1 values are typically distributed over more than 1 order of magnitude at low T ; that is, σ_{\log} reaches a value of ≈ 1.5 at $T = T_g^{\text{NMR}}$. This width does not depend strongly on the number of holes since similar values of σ_{\log} are observed for $x=0.10$ (Ref. 18; Fig. 6) and $x=0.06$ (Ref. 28; not shown) at $T \approx T_g^{\text{NMR}}$.

Strikingly, the same value of $\sigma_{\log} \approx 1.5$ is found at $T = T_g^{\text{NMR}}$ in both pristine and disordered samples for $x=0.12$ [Fig. 6(c)]. Thus, the distribution width appears to be insensitive to an $\sim 1\%$ of in-plane disorder as well. One could argue that this result can be explained by the fact that

$\text{La}_{1.88}\text{Sr}_{0.12}\text{CuO}_4$ is already a significantly disordered material in its pristine version. However, this argument does not hold since a typical 1% of nonmagnetic impurities or vacancies is highly detrimental to T_c and it clearly affects other magnetic properties as well.¹⁵

Finally, we will comment on alternative explanations of the stretched-exponential behavior of the NMR relaxation. It was suggested that the inhomogeneous magnetic state is related to extended charge-density waves with imaginary order parameter (*id*-CDW).³⁴ Within this model, the observed inhomogeneity in the NMR and μSR quantities would originate from sliding motions of orbital currents coexisting with the *d*-wave superconducting state. It is known that any order parameter of *d*-wave symmetry should be highly sensitive to impurities. This is in contrast to our data, showing that the inhomogeneity of ^{139}Tl is insensitive to 1% of atomic disorder. Therefore, the *id*-CDW scenario is unlikely to account for our observations.

Furthermore, a power-law time dependence of the spin-spin correlation function, instead of a distribution, is also debated in canonical spin glasses as an explanation for the stretched-exponential NMR or μSR relaxation.³⁵ Anyhow, we did not consider this possibility as the presence of magnetic heterogeneity in $\text{La}_{2-x}\text{Sr}_x\text{CuO}_4$ is established by various experimental facts, such as the partial wipeout of the NMR signal or the *T*-dependent broadening of the NMR linewidth.

VIII. CONCLUSION

We have presented an NMR investigation of $\text{La}_{1.88}\text{Sr}_{0.12}\text{CuO}_4$, a prototypical material for studying spin-glass and stripe-ordering instabilities in the superconducting regime. Our analysis can be viewed as a parametrization of the stretched-exponential spin-lattice relaxation of ^{139}La nuclei. We observe that this phenomenon is not affected by an $\sim 1\%$ level of disorder. This result might thus support proposals¹² of heterogeneous dynamics, or more generally of glassiness, which is not due to quenched disorder. However, how much of the magnetic heterogeneity/glassiness of $\text{La}_{2-x}\text{Sr}_x\text{CuO}_4$ is attributable to nanoscale variation of the hole doping remains unclear. It would also be interesting to investigate whether our results for the special $x=0.12$ material still hold in samples with lower Sr concentration, including the nonsuperconducting cluster spin-glass region of the phase diagram. The glassy nature of magnetism in superconducting cuprates clearly calls for further theoretical and experimental consideration, especially given the recent observation of an electronic glass by scanning tunneling microscopy.³⁶

ACKNOWLEDGMENTS

We acknowledge useful communications with Roberto de Renzi and Jeff Sonier.

*Corresponding author; marc-henri.julien@ujf-grenoble.fr

¹For $\text{La}_{2-x}\text{Sr}_x\text{CuO}_4$, see M.-H. Julien, *Physica B* (Amsterdam) **329-333**, 693 (2003), and references therein.

²Other cases in *p*-type cuprates are $\text{YBa}_{2-x}\text{Ca}_x\text{Cu}_3\text{O}_{6+y}$ [C. Niedermayer, C. Bernhard, T. Blasius, A. Golnik, A. Moodenbaugh, and J. I. Budnick, *Phys. Rev. Lett.* **80**, 3843 (1998)]; $\text{Ca}_x\text{La}_{1-x}\text{Ba}_{1.75-x}\text{La}_{0.25+x}\text{Cu}_3\text{O}_y$ [Amit Kanigel, Amit Keren, Yaakov Eckstein, Arkady Knizhnik, James S. Lord, and Alex Amato, *ibid.* **88**, 137003 (2002)]; $\text{Bi}_{2.1}\text{Sr}_{1.9}\text{Ca}_{1-x}\text{Y}_x\text{Cu}_2\text{O}_{8+y}$ [C. Panagopoulos, J. L. Tallon, B. D. Rainford, T. Xiang, J. R. Cooper, and C. A. Scott, *Phys. Rev. B* **66**, 064501 (2002)]; $\text{YBa}_2\text{Cu}_3\text{O}_{6+y}$ [R. F. Kiefl, J. H. Brewer, J. Carolan, P. Dosanjh, W. N. Hardy, R. Kadono, J. R. Kempton, R. Krahn, P. Schleger, B. X. Yang, Hu Zhou, G. M. Luke, B. Sternlieb, Y. J. Uemura, W. J. Kossler, X. H. Yu, E. J. Ansaldo, H. Takagi, S. Uchida, and C. L. Seaman, *Phys. Rev. Lett.* **63**, 2136 (1989); S. Sanna, G. Allodi, G. Concas, A. D. Hillier, and R. De Renzi, *ibid.* **93**, 207001 (2004); R. I. Miller, R. F. Kiefl, J. H. Brewer, F. D. Callaghan, J. E. Sonier, R. Liang, D. A. Bonn, and W. Hardy, *Phys. Rev. B* **73**, 144509 (2006)]; and $\text{Ca}_{2-x}\text{Na}_x\text{CuO}_2\text{Cl}_2$ [K. Ohishi, I. Yamada, A. Koda, W. Higemoto, S. R. Saha, R. Kadono, K. M. Kojima, M. Azuma, and M. Takano, *J. Phys. Soc. Jpn.* **74**, 2408 (2005)].

³H.-H. Klauss, *J. Phys.: Condens. Matter* **16**, S4457 (2004), and references therein.

⁴S. A. Kivelson and V. J. Emery, *Stripes and Related Phenomena* (Kluwer, Dordrecht/Plenum, New York, 2000), p. 91.

⁵T. Suzuki, T. Goto, K. Chiba, T. Shinoda, T. Fukase, H. Kimura, K. Yamada, M. Ohashi, and Y. Yamaguchi, *Phys. Rev. B* **57**,

R3229 (1998).

⁶H. Kimura, K. Hirota, H. Matsushita, K. Yamada, Y. Endoh, S.-H. Lee, C. F. Majkrzak, R. Erwin, G. Shirane, M. Greven, Y. S. Lee, M. A. Kastner, and R. J. Birgeneau, *Phys. Rev. B* **59**, 6517 (1999).

⁷S. Wakimoto, R. J. Birgeneau, Y. S. Lee, and G. Shirane, *Phys. Rev. B* **63**, 172501 (2001).

⁸J. M. Tranquada, N. Ichikawa, and S. Uchida, *Phys. Rev. B* **59**, 14712 (1999).

⁹B. M. Andersen, P. J. Hirschfeld, A. P. Kampf, and M. Schmid, *Phys. Rev. Lett.* **99**, 147002 (2007); see also the most recent works on the spin-glass phase: O. Parcollet and A. Georges, *Phys. Rev. B* **59**, 5341 (1999); K. S. D. Beach and R. J. Gooding, *Eur. Phys. J. B* **16**, 579 (2000); N. Hasselmann, A. H. Castro Neto, and C. M. Smith, *Phys. Rev. B* **69**, 014424 (2004); G. Alvarez, M. Mayr, A. Moreo, and E. Dagotto, *ibid.* **71**, 014514 (2005); A. Lüscher, A. I. Milstein, and O. P. Sushkov, *Phys. Rev. Lett.* **98**, 037001 (2007).

¹⁰P. M. Singer, A. W. Hunt, and T. Imai, *Phys. Rev. Lett.* **88**, 047602 (2002); P. M. Singer, T. Imai, F. C. Chou, K. Hirota, M. Takaba, T. Kakeshita, H. Eisaki, and S. Uchida, *Phys. Rev. B* **72**, 014537 (2005); See also J. Haase, C. P. Slichter, R. Stern, C. T. Milling, and D. G. Hinks, *Physica C* **341-348**, 1727 (2000); H. J. Grafe, N. J. Curro, M. Hücker, and B. Büchner, *Phys. Rev. Lett.* **96**, 017002 (2006).

¹¹N. J. Curro, P. C. Hammel, B. J. Suh, M. Hücker, B. Büchner, U. Ammerahl, and A. Revcolevschi, *Phys. Rev. Lett.* **85**, 642 (2000); See also B. J. Suh, P. C. Hammel, M. Hücker, B. Büchner, U. Ammerahl, and A. Revcolevschi, *Phys. Rev. B* **61**,

- R9265 (2000); B. Simovič, P. C. Hammel, M. Hückler, B. Büchner, and A. Revcolevschi, *ibid.* **68**, 012415 (2003).
- ¹²H. Westfahl, J. Schmalian, and P. G. Wolynes, *Phys. Rev. B* **68**, 134203 (2003), and references therein; See also partially related ideas in M. P. Kennett, C. Chamon, and L. F. Cugliandolo, *ibid.* **72**, 024417 (2005); and phenomenological considerations in C. Panagopoulos and V. Dobrosavljević, *ibid.* **72**, 014536 (2005).
- ¹³A. W. Hunt, P. M. Singer, A. F. Cederström, and T. Imai, *Phys. Rev. B* **64**, 134525 (2001); See also G. B. Teitelbaum, I. M. Abu-Shiekah, O. Bakharev, H. B. Brom, and J. Zaanen, *ibid.* **63**, 020507(R) (2000).
- ¹⁴S. Katano, M. Sato, K. Yamada, T. Suzuki, and T. Fukase, *Phys. Rev. B* **62**, R14677 (2000).
- ¹⁵Y. Koike, A. Kobayashi, T. Kawaguchi, M. Kato, T. Noji, Y. Ono, T. Hikita, and Y. Saito, *Solid State Commun.* **82**, 889 (1992); T. Adachi, S. Yairi, K. Takahashi, Y. Koike, I. Watanabe, and K. Nagamine, *Phys. Rev. B* **69**, 184507 (2004); S. Komiya and Y. Ando, *ibid.* **70**, 060503(R) (2004).
- ¹⁶M. H. Julien, T. Fehér, M. Horvatić, C. Berthier, O. N. Bakharev, P. Ségransan, G. Collin, and J. F. Marucco, *Phys. Rev. Lett.* **84**, 3422 (2000).
- ¹⁷F. Rullier-Albenque, H. Alloul, and R. Tourbot, *Phys. Rev. Lett.* **87**, 157001 (2001).
- ¹⁸M.-H. Julien, A. Campana, A. Rigamonti, P. Carretta, F. Borsa, P. Kuhns, A. P. Reyes, W. G. Moulton, M. Horvatić, C. Berthier, A. Vietkin, and A. Revcolevschi, *Phys. Rev. B* **63**, 144508 (2001).
- ¹⁹A. T. Savici, Y. Fudamoto, I. M. Gat, T. Ito, M. I. Larkin, Y. J. Uemura, G. M. Luke, K. M. Kojima, Y. S. Lee, M. A. Kastner, R. J. Birgeneau, and K. Yamada, *Phys. Rev. B* **66**, 014524 (2002).
- ²⁰A. T. Savici, A. Fukaya, I. M. Gat-Malureanu, T. Ito, P. L. Russo, Y. J. Uemura, C. R. Wiebe, P. P. Kyriakou, G. J. MacDougall, M. T. Rovers, G. M. Luke, K. M. Kojima, M. Goto, S. Uchida, R. Kadono, K. Yamada, S. Tajima, T. Masui, H. Eisaki, N. Kaneko, M. Greven, and G. D. Gu, *Phys. Rev. Lett.* **95**, 157001 (2005).
- ²¹L. H. Machtoub, B. Keimer, and K. Yamada, *Phys. Rev. Lett.* **94**, 107009 (2005).
- ²²A. Narath, *Phys. Rev.* **162**, 320 (1967).
- ²³V. F. Mitrović, E. E. Sigmund, M. Eschrig, H. N. Bachman, W. P. Halperin, A. P. Reyes, P. Kuhns, and W. G. Moulton, *Nature (London)* **413**, 501 (2001).
- ²⁴D. C. Johnston, *Phys. Rev. B* **74**, 184430 (2006).
- ²⁵N. Bloembergen, E. M. Purcell, and R. V. Pound, *Phys. Rev.* **73**, 679 (1948).
- ²⁶The real onset of slowing down might occur at a somewhat higher temperature, if it is masked by a T -dependent quadrupolar contribution to $^{139}\text{T}_1$.
- ²⁷J. H. Cho, F. Borsa, D. C. Johnston, and D. R. Torgeson, *Phys. Rev. B* **46**, 3179 (1992).
- ²⁸M.-H. Julien, F. Borsa, P. Carretta, M. Horvatić, C. Berthier, and C. T. Lin, *Phys. Rev. Lett.* **83**, 604 (1999).
- ²⁹S. Chakravarty and R. Orbach, *Phys. Rev. Lett.* **64**, 224 (1990).
- ³⁰G. B. Teitel'baum, V. E. Kataev, E. L. Vavilova, P. L. Kuhns, A. P. Reyes, and W. G. Moulton, *JETP Lett.* **78**, 726 (2003).
- ³¹Substituting this number for $(T_1^{-1})_{\text{max}}$ into Eq. (4) yields the reasonable value of $\langle h_{\perp}^2 \rangle^{1/2} \approx 0.5$ kOe [I. Watanabe, *J. Phys. Soc. Jpn.* **63**, 1560 (1994)].
- ³²A. W. Hunt, P. M. Singer, K. R. Thurber, and T. Imai, *Phys. Rev. Lett.* **82**, 4300 (1999).
- ³³J. Bobroff, H. Alloul, S. Ouazi, P. Mendels, A. Mahajan, N. Blanchard, G. Collin, V. Guillen, and J.-F. Marucco, *Phys. Rev. Lett.* **89**, 157002 (2002).
- ³⁴M. Eremin and A. Rigamonti, *Phys. Rev. Lett.* **88**, 037002 (2002).
- ³⁵A. Keren, G. Bazalitsky, I. Campbell, and J. S. Lord, *Phys. Rev. B* **64**, 054403 (2001); X. Zong, A. Niazi, F. Borsa, X. Ma, and D. C. Johnston, *ibid.* **76**, 054452 (2007).
- ³⁶Y. Kohsaka, C. Taylor, K. Fujita, A. Schmidt, C. Lupien, T. Hanaguri, M. Azuma, M. Takano, H. Eisaki, H. Takagi, S. Uchida, and J. C. Davis, *Science* **315**, 1380 (2007).